Available online at www.sciencedirect.com

SciVerse ScienceDirect

journal homepage: www.elsevier.com/locate/jmbbm

Research paper

Micromechanical analysis of native and cross-linked collagen type I fibrils supports the existence of microfibrils

L. Yang[a], K.O. van der Werf[b], P.J. Dijkstra[a], J. Feijen[a], M.L. Bennink[b,*]

[a] Polymer Chemistry and Biomaterials, Faculty of Science & Technology and Institute for Biomedical Technology and Technical Medicine (MIRA), University of Twente, P.O. Box 217, 7500 AE, Enschede, The Netherlands

[b] Nanobiophysics, Faculty of Science & Technology and MESA + Institute for Nanotechnology, University of Twente, P.O. Box 217, 7500 AE, Enschede, The Netherlands

ARTICLE INFO

Article history:
Received 8 August 2011
Received in revised form
10 November 2011
Accepted 16 November 2011
Published online 25 November 2011

Keywords:
Collagen
Microstructure
Mechanical properties
AFM (atomic force microscopy)

ABSTRACT

The mechanical properties of individual collagen fibrils of approximately 200 nm in diameter were determined using a slightly adapted AFM system. Single collagen fibrils immersed in PBS buffer were attached between an AFM cantilever and a glass surface to perform tensile tests at different strain rates and stress relaxation measurements. The stress–strain behavior of collagen fibrils immersed in PBS buffer comprises a toe region up to a stress of 5 MPa, followed by the heel and linear region at higher stresses. Hysteresis and strain-rate dependent stress–strain behavior of collagen fibrils were observed, which suggest that single collagen fibrils have viscoelastic properties. The stress relaxation process of individual collagen fibrils could be best fitted using a two-term Prony series. Furthermore, the influence of different cross-linking agents on the mechanical properties of single collagen fibrils was investigated. Based on these results, we propose that sliding of microfibrils with respect to each other plays a role in the viscoelastic behavior of collagen fibrils in addition to the sliding of collagen molecules with respect to each other. Our finding provides a better insight into the relationship between the structure and mechanical properties of collagen and the micro-mechanical behavior of tissues.

1. Introduction

The mechanical properties of tissues like tendons, ligaments, and bone are directly related to the arrangement of their constituent components. Collagen type I is the most abundant protein in the human body, and is the principal, tensile stress-bearing component, crucial for the strength and stability of a wide range of tissues. In this fibrillar type collagen the collagen triple helices, also called collagen molecules, are assembled in fibrils and cross-linked via the amino acids lysine and hydroxyl lysine present in their telopeptide regions (Silver et al., 2003; Ottani et al., 2002). The fibrils in turn are assembled in fibers, which depending on the type of tissue are assembled in fascicles like in tendon. The existence of other sub-structures in collagen fibrils has been debated for years. The *D*-periodic five-stranded microfibril, an assembly of five triple helices as a sub-structure, was first proposed by Smith (1968). Some recent studies suggest the presence of these microfibrils in fibrils. A longitudinal

* *Corresponding author.* Tel.: +31 53 4896800; fax: +31 53 4891105.
E-mail address: m.l.bennink@utwente.nl (M.L. Bennink).

1751-6161/$ - see front matter © 2011 Elsevier Ltd. All rights reserved.
doi:10.1016/j.jmbbm.2011.11.008

microfibrillar structure with a width of 4–8 nm was visualized in both hydrated (Raspanti et al., 2001; Habelitz et al., 2002) and dehydrated (Baselt et al., 1993) collagen type I fibrils using tapping mode AFM imaging. Three-dimensional image reconstructions of 36 nm-diameter corneal collagen fibrils also showed a 4 nm repeat in a transverse section, which was ascribed to the microfibrillar structure (Holmes et al., 2001). Using X-ray diffraction culminating in an electron density map, Orgel et al. (2006) suggested the presence of right-handed supertwisted microfibrillar structures in collagen fibrils.

As this hierarchical organization of collagen was revealed, many studies were initiated in an attempt to understand the relation between this structure and the mechanical properties as measured for tissue (Silver et al., 2003; Ottani et al., 2002; Puxkandl et al., 2002; Hulmes, 2002; Mosler et al., 1985; Sasaki and Odajima, 1996; Wang, 2006; Dowling and Dart, 2005; Magnusson et al., 2003; Silver et al., 2000). In this respect, it is of utmost importance to obtain the mechanical behavior of collagen fibrils, and to determine its contribution to the overall mechanical behavior of tissues. Stress–strain curves of collagen fibers and those of collagen-based tissues (such as tendon) in a hydrated state reveal a typical low stress, or 'toe' region, at low strains (<2%), followed by a 'heel' region where the slope slowly increases, and then followed by a linear region at higher strains (>3%) (Silver et al., 2003). Experimentally determined elastic moduli are typically between 0.1 and 1 GPa for these fibers and tissues (Butler et al., 1986; An et al., 2004; Pins and Silver, 1995). Applying tensile testing combined with synchrotron radiation diffraction on tissue samples, Mosler and co-workers (Mosler et al., 1985; Folkhard et al., 1987a,b) suggested that stretching of the collagen molecules and their sliding with respect to each other are the two major mechanisms to account for the elongation of collagen fibrils. This also forms the basis for the basis for simulation work done by Buehler (2006, 2008). In recent years, the development of micro- and nanomanipulation techniques like the atomic force microscope (AFM), offers a novel and direct means to measure the mechanical properties of materials on a micro- and nanometer scale (Smith et al., 2006; Kis et al., 2002; Guzmán et al., 2006; Oliver and Pharr, 2004), for example in the case of stretching individual DNA and protein molecules (Fisher et al., 1999; Carrion-Vazquez et al., 2000). With respect to collagen-based materials, studies have been initiated on the mechanical properties of individual collagen fibrils (10–500 nm in diameter) (Thompson et al., 2001; Graham et al., 2004; van der Rijt et al., 2006; Eppell et al., 2006; Strasser et al., 2007; Wenger et al., 2007; Svennson et al., 2010; Svensson et al., 2010). Most of the reported tests are limited to low strain ranges of typically a few percent, which provide very little information on the possible mechanism of the mechanical behavior of collagen fibrils. Eppel and coworkers have developed a specific MEMS device for tensile testing individual collagen molecules, that allows testing up to strains of 100% (Shen et al., 2008). Tests up to these strains are sufficient to break the fibrils, and thus determine the stress and strain at break. Although the presence of viscoelasticity of individual collagen fibrils was expected and has been observed by many researchers already, it had not been discussed and/or quantified in detail. Only recently, Svensson et al. studied this viscous behavior in more detail (Svensson et al., 2010). By stretching individual human patellar tendon fibrils at different strain rates and comparing the stress–strain curves with one recorded using a step-wise stress relaxation test (zero strain rate), the authors have separated the elastic and viscous component. Shen et al. using a microelectromechanical systems platform, performed in vitro coupled creep and stress relaxation tests on collagen fibrils isolated from the sea cucumber dermis (Shen et al., 2011). The time dependent behavior fitted well assuming a relaxation process described with two time constants.

In our recent research, we have measured the stress–strain behavior and time dependent mechanical properties of single native and crosslinked collagen fibrils to get more information on the viscoelastic behavior of the fibrils. Tensile tests at different strain rates and stress relaxation measurements of collagen fibrils have been performed using a home-built AFM system which has been adapted to allow stretching of collagen fibrils (initial length between 40 and 100 μm) up to 400 μm. The micro-tensile tests and stress relaxation measurements of collagen fibrils were performed on native fibrils and fibrils either cross-linked with 1-ethyl-3-(3-dimethyl aminopropyl) carbodiimide hydrochloride (EDC) or glutaraldehyde. Cross-linking with EDC results in "zero-length" cross-links, which in the case of collagen will lead to additional inter- and intra-molecular cross-links within the collagen fibrils (Olde Damink et al., 1996; Everaerts et al., 2007). Cross-linking with glutaraldehyde, however, introduces cross-links which can be at least 1.3 nm in length, leading to not only intra- and inter-molecular cross-links but also cross-links between microfibrils (Olde Damink et al., 1995). The differences obtained in the viscoelastic properties of these two differently cross-linked collagen fibrils, does not only provide additional evidence for the existence of microfibrils in the collagen fibril, but also indicates that the microfibrillar structure contributes significantly to the viscoelastic behavior of collagen fibrils.

2. Materials and methods

2.1. *Sample preparation for micro-tensile tests*

The general procedure for the isolation of (non)cross-linked collagen fibrils was described previously (Yang et al., 2008, 2007). In brief, a suspension of collagen fibrils was prepared from bovine Achilles tendon collagen type I (Sigma-Aldrich, Steinheim, Germany) by homogenization and filtration. Analysis of this suspension showed a high concentration of collagen fibrils. FTIR and DSC analysis indicated that these fibrils were not denatured in the isolation process (Yang et al., 2008). We therefore use the term native collagen fibrils. This suspension was further diluted to obtain a suitable suspension (~1 mg/ml) for depositing individual fibrils on a substrate, that are not crossing one another.

Furthermore, suspensions containing chemically cross-linked fibrils were prepared. Cross-linking of the fibrils was performed in the diluted suspensions (to avoid cross-linking

between the fibrils) using either the water-soluble carbodiimide 1-ethyl-3-(3-dimethyl-aminopropyl) carbodiimide hydrochloride (EDC) in the presence of N-hydroxysuccinimide (NHS) or glutaraldehyde as previously described (Yang et al., 2008, 2007). The degree of cross-linking of the collagen fibrils is related to the increase in the denaturation (shrinkage) temperature (T_d) and decrease of free amino group content after cross-linking. T_d values were determined by DSC (DSC 7, Perkin Elmer, Norwalk, CT, USA). Free amino group contents of native and cross-linked samples were determined using the 2, 4, 6-trinitrobenzenesulfonic acid (TNBS) assay (Yang et al., 2007).

Deposition of single collagen fibrils on partly Teflon (Teflon AF, 1601S Dupont, Wilmington, DE, USA) coated glass substrates (Microscope cover glasses, Ø = 15 mm, Marlenfeld GmbH, Germany) has been described in detail in our previous work (van der Rijt et al., 2006).

2.2. AFM imaging

To determine the diameter and morphology of collagen fibrils, AFM measurements were carried out with the same AFM in tapping mode using V-shaped Si_3O_4 cantilevers (coated sharp micro-levers MSCT-AUHW, type F, spring constant k = 0.5 N/m, Veeco, Cambridge, UK). At ambient conditions, a tapping frequency of ~120 kHz and a tapping amplitude of ~400–600 nm were used.

2.3. Micro-tensile tests of individual collagen fibrils

A collagen fibril was fixed between the end of an AFM cantilever (Multi 130 A, k = 35 N/m Veeco, Dourdan, France) and the glass surface by small glue droplets (Two-component glue, Araldite 2011, Vantico, Basel, Switzerland) (van der Rijt et al., 2006). The AFM cantilever was then moved to a position above the glue droplet on the glass surface to ensure that the stretching of the fibril is in a vertical direction. After this, the sample holder was moved downward by a 400 μm piezo-based positioning stage (nanoMIPOS 400, Piezosystem Jena, Jena, Germany) until a ~4 nN deflection signal of the AFM cantilever was reached. The distance between the AFM tip and the glass surface at this point was defined as the initial length of the fibril (L_0). To obtain calibrated force data, the sensitivity of the AFM system with the cantilever, i.e. the ratio between the bending of the cantilever and the deflection as measured by the quadrant detector, needs to be determined. This was done by recording a force-distance curve with this tip on a glass surface in PBS buffer conditions. In order not to risk any damage to the attached collagen fibril by pressing the tip against the glass, this calibration is done after the tensile tests of the collagen fibril.

A saw-tooth loading pattern was provided using the calibrated 400 μm piezo-based stage controlled by LabView (Version 6.1, National Instruments, Austin, Texas, USA). Individual collagen fibrils were extended at different strain rates ranging from 0.1 to 10 μm/s. For tensile tests of fibrils in PBS buffer, the collagen fibrils already fixed between the AFM cantilever and the glass surface were immersed in ~1 ml PBS buffer and left to equilibrate for 15 min before starting the tensile tests. Longer equilibration times did not lead to changes in the results of the micro-tensile tests, indicating that the collagen fibrils were fully rehydrated. The elasticity modulus of the collagen fibrils was derived from the maximum slope of the stress–strain curves.

Using the AFM in force distance mode provides force versus extension data. Calibration of the force was done by determining the spring constant of each tip-less cantilever by pushing it against a pre-calibrated cantilever as described elsewhere (Torii et al., 1996). Before tensile testing a fibril, the cross-sectional area of the fibril was determined from tapping mode AFM images made at different positions along the fibril. Knowing the force (F) applied on the cantilever, the length (L) and the cross-sectional area (A) of the fibril, the force versus extension data were converted into stress (σ) versus strain (ε) data, using:

$$\sigma = \frac{F}{A} \quad \text{and} \quad \varepsilon = \frac{L - L_0}{L} \cdot 100\% \tag{1}$$

where L_0 is the initial length of the collagen fibril.

In case multiple tensile tests were performed on the same fibril at forces high enough to lead to irreversible lengthening, the length (L) of the fibril and its cross-sectional area (A) were corrected after each cycle of loading, in order to correctly calculate the stress–strain behavior. For irreversible lengthening of the fibril with ΔL, the new length of the fibril is $L = L_0 + \Delta L$, where L_0 is the length of the fibril during the previous test. The new cross-section is then $A = A_0 \cdot L_0/L$, where A_0 is the cross-section during the previous tensile test experiment.

2.4. Stress relaxation measurements

Individual collagen fibrils were loaded to approximately 5%–7% strain at a loading rate of 4 μm/s. Then, the strain was maintained constant and the stress was recorded during a 5–10 min period. The reduction in stress during this experiment results in a change in the deflection of the cantilever, and thus a slight increase in the length of the fibril, but this is very small in comparison with the total length of the fibril and therefore neglected. The stress was measured from the moment the strain was kept constant. The normalized stress $\sigma(t)/\sigma(0)$ as a function of time was fitted to a one-, two- and three-term Prony series model (Wineman and Rajagopal, 2000) and is expressed by:

$$g(t) = \frac{\sigma(t)}{\sigma(0)} = 1 - \sum_i A_i(1 - e^{-t/\tau_i}) \tag{2}$$

where $g(t)$ is the normalized stress at time t, and i is the number of terms taken into the Prony series. The dimensionless prefactors A_i, relaxation times τ_i are the parameters left variable in the fitting procedure.

3. Results and discussion

3.1. Sample preparation and characterization

Incubating partly Teflon coated glass substrates in a highly diluted collagen suspension (~1 mg/ml) gave a sufficient amount of fully separated collagen fibrils that crossed the

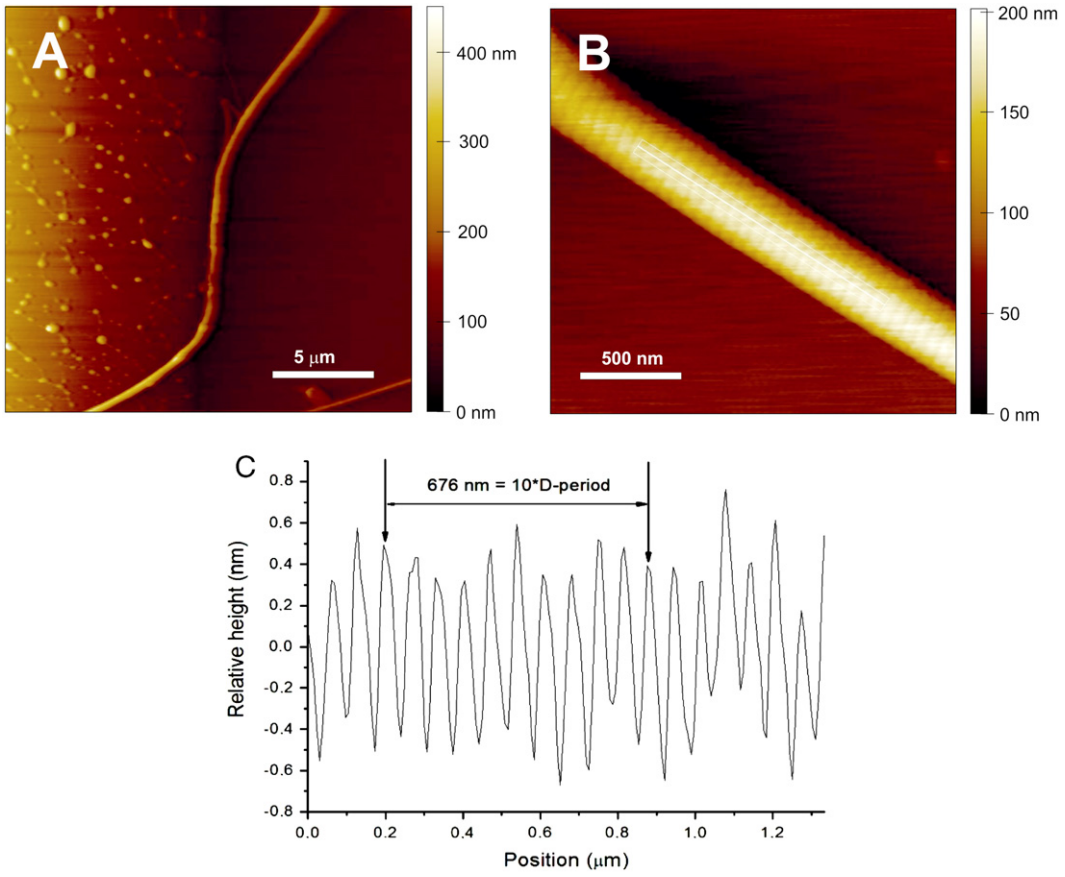

Fig. 1 – (A) AFM image of a collagen type I single fibril deposited on a Teflon–glass interface. The surface of the left part of the image is glass coated with Teflon. (B) AFM image of a collagen type I single fibril. (C) Averaged line section, created by averaging 11 parallel line sections along the fibril axis, as indicated by the white box in (B). *D*-period is clearly visible in the AFM image as a modulation with a depth of about 1 nm (line section has been flattened). The periodicity found for this fibril is 67.6 nm.

Teflon–glass boundary. Using the inverted optical microscope, sufficiently long (40–100 μm) and uniformly shaped fibrils were selected for mechanical testing. In a next step atomic force microscopy imaging was used to image the fibrils to verify the presence of the characteristic *D*-period of 67 nm and the uniformity of the fibril structure on the nanometer scale. An AFM image of an individual collagen fibril crossing the Teflon–glass boundary is presented in Fig. 1(A). The Teflon–glass boundary is clearly visible in the image. The Teflon layer has a thickness of 500 ± 200 nm. Fig. 1(B) is a zoom of the collagen fibril that clearly reveals the 67 nm *D*-period.

Glutaraldehyde cross-linking has been widely applied for the stabilization of e.g. tissue heart valves. Activation methods used in polypeptide chemistry like EDC/NHS are well known to cross-link collagen and have the advantage to overcome problems associated with glutaraldehyde toxicity (Olde Damink et al., 1996). The two methods were used to cross-link collagen fibrils and in both cases the *D*-period of 67 nm was observed using AFM imaging. The degree of cross-linking was determined through the change in denaturation temperature (T_d) and free amino group content (n/1000) as a result of the cross-linking reaction. The T_d of the native fibrils was 55.0 °C and increased to 75.0 °C after cross-linking with EDC/NHS. The free amino group content decreased from 28 per 1000 amino acids to a value of 9. After cross-linking with glutaraldehyde, the denaturation temperature increased to 76.0 °C and the primary amino group content decreased to a value of 8/1000 amino acids. According to our previous finding (Olde Damink et al., 1996, 1995) these results indicate a high degree of cross-linking.

3.2. *Stress–strain curves of individual native collagen fibrils*

After fixation between the AFM cantilever and the glass surface using small glue droplets (see details in Fig. 2), the collagen fibril was straightened to its initial length by adjusting the position of the AFM cantilever and the height of the sample holder manually. The length of the attached collagen fibrils ranged from 40 to 100 μm. A calibrated piezo-based positioning stage with a maximum extension distance of 400 μm was added to the AFM setup, allowing the sample holder to move over that distance in a controlled manner. This enabled the collagen fibrils to be stretched to larger

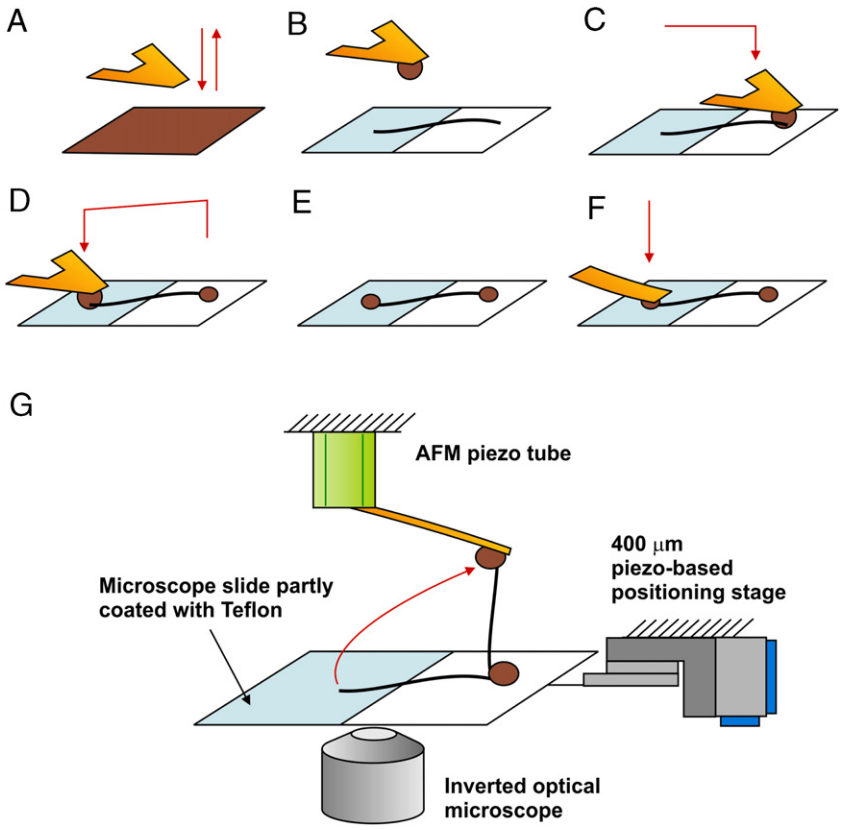

Fig. 2 – Schematic drawing of the procedure of attaching an individual collagen fibril between the AFM cantilever and the partly Teflon coated glass surface. (A) Two component epoxy glue was mixed and spread onto a microscope glass surface. A triangular AFM cantilever was dipped into the layer of glue to get a droplet at the end of the cantilever. (B) Using the optical microscope, a collagen fibril crossing the glass–Teflon boundary was selected. (C) The glue-dipped tip was moved to the end of the collagen fibril on glass to deposit a small droplet. (D) Similarly, a glue droplet was put onto the other end of the fibril. (E) The cantilever was replaced with a rectangular one from which the tip has been removed. (F) The end of the cantilever was brought into contact with the last deposited glue droplet, and left there for 12 h. (G) The cantilever was carefully raised from the surface. The non-sticking property of Teflon makes the collagen fibril end stick to the AFM cantilever and ready for the micro-tensile testing. A 400 μm piezo-based positioning stage connected to the sample holder was used to allow large extensions (i.e. strain) of the fibril.

percentages of strain and even to the breakage of the collagen fibril.

To mechanically test a fibril in the hydrated state, a collagen fibril fixed between the AFM cantilever and the glass surface was fully immersed in PBS buffer. The diameter of the fibrils (the height of the fibril in AFM imaging) increased by ~50% upon hydration in PBS buffer using tapping mode AFM imaging. Measuring the force applied on the cantilever, the length and the cross-sectional area of the fibril, stress–strain curves of individual collagen fibrils could be derived (see Materials and Methods). Stress–strain curves obtained from stretching collagen fibrils up to different maximum strains are presented in Fig. 3.

A toe region at low strain was found, followed by a heel region and then by a linear region at higher strains. This 'toe' region is consistent with recently published computational work of Gautieri et al. (2011) that shows that the straightening of twisted networks in the monomer is responsible for this part of the stress–strain behavior. These stress–strain curves reflect the typical stress–strain behavior of collagen-based tissues and fibers (Wang, 2006). In the toe and heel region, the slope of the stress–strain curves increased continuously up to ~3% strain. From this point on, the stress–strain behavior of the fibril was linear and an elasticity modulus of 0.6± 0.2 GPa ($n = 11$) was calculated from the maximum slope of the stress–strain curves. This value is in the same range of 0.1 to 1 GPa as reported for tendons and collagen fibers in a hydrated state (Butler et al., 1986; An et al., 2004; Pins and Silver, 1995). The toe and heel regions could be ascribed to the straightening of kinks in the collagen molecules caused by hydration (Misof et al., 1997). The failure of all tested native collagen fibrils ($n = 11$) occurred at 11%–15% strain with a stress at break of 60 ± 10 MPa. It should be noted that the fibrils never failed at the glue fixation points, which was verified by optical microscopy. The mechanical behavior of the fibrils was reversible below ~6% strain (Fig. 3(A)). At higher strain levels hysteresis in the stress–strain curves of the fibrils was found (Fig. 3(B)).

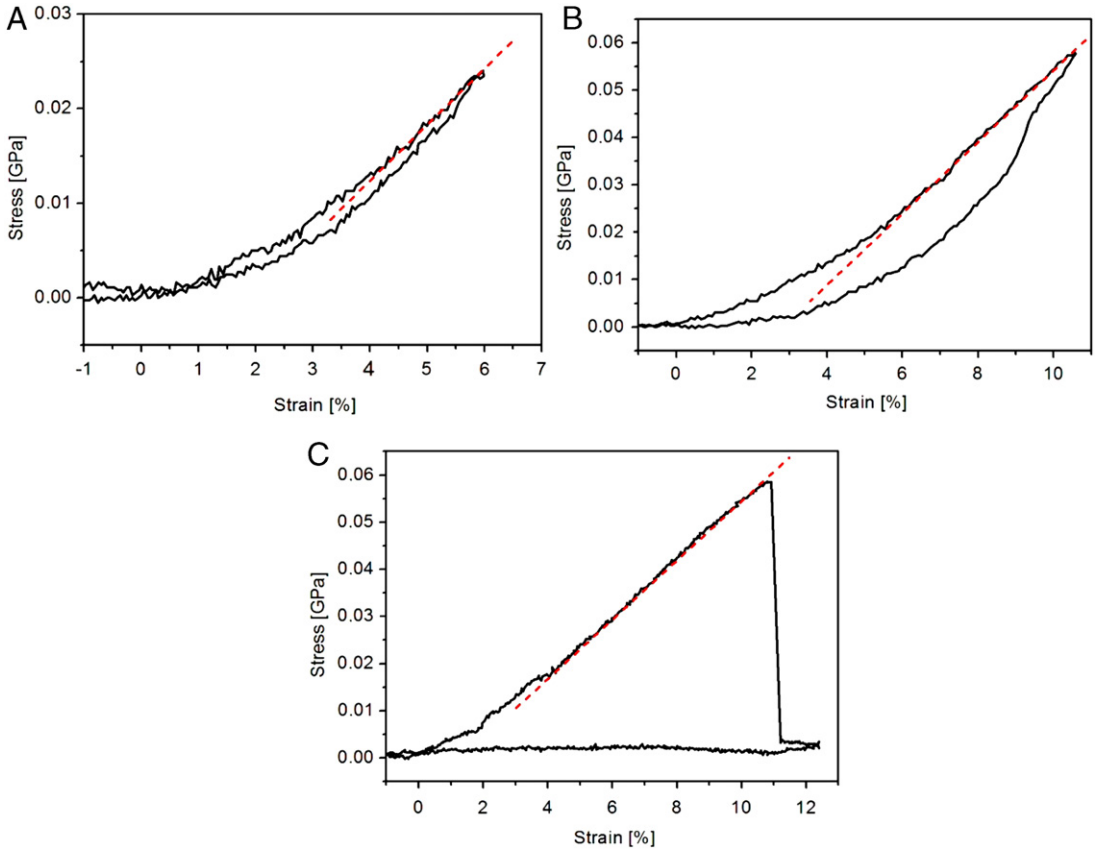

Fig. 3 – Representative stress–strain curves of individual collagen type I fibrils in PBS buffer up to 6% (A), 10% (B) and 11% (C) strain. The strain rate in all stretching-relaxation cycles was 4 μm/s. The elasticity modulus of the fibril was determined from the maximum slope of the stress–strain curve as indicated with a red dashed line. The stress–strain behavior was fully reversible at low strain levels (below 6%) (A). Hysteresis of the collagen fibril was observed from the stress–strain plots especially at higher strain levels (B). Failure of the fibril occurred at 11% strain with a stress of 0.06 GPa (C). The tested fibril is 50 ± 2 μm in length and 305 ± 10 nm in diameter. (For interpretation of the references to colour in this figure legend, the reader is referred to the web version of this article.)

3.3. *Influence of cross-linking on the stress–strain behavior*

For biomedical applications of collagen-based materials chemical cross-linking of collagen is important. It is an efficient method to retard the degradation by enzymes like collagenase and also to inhibit immunological reactions. Commonly used cross-linkers for collagen are glutaraldehyde and activation methods using water-soluble carbodiimide like EDC. It is known that cross-linkers do affect the mechanical properties of collagen-based materials (Olde Damink et al., 1996; Everaerts et al., 2007; Olde Damink et al., 1995) but this effect on single collagen fibrils has not been studied in detail.

Stress–strain curves have been measured for individual collagen fibrils fully immersed in PBS buffer cross-linked with EDC/NHS (Fig. 4(A)) and glutaraldehyde (Fig. 4(B)). The shape of the stress–strain curves was similar to those of native collagen fibrils. The slope of the stress–strain curves increased up to 5%–6% strain. Above a strain of ~10% hysteresis and irreversible lengthening of the fibril was observed for both cross-linking agents. The elasticity moduli determined for the differently cross-linked fibrils, however were quite different. For EDC/NHS cross-linked fibrils, the average elasticity modulus of the tested fibrils was 700 ± 100 MPa, which was comparable to native fibrils. For fibrils cross-linked with glutaraldehyde in PBS buffer, a ~3 times higher modulus was found compared to the value for native fibrils.

Having the ability to stretch the fibril to 400 μm, allowed to elongate up to the point that the fibril breaks. For native collagen fibrils the average stress at break was 60 MPa at a strain of 13%. Collagen fibrils cross-linked with either one of the agents revealed a strain at break and failure stress higher than those obtained for native fibrils (Table 1). From the results presented here it can be concluded that the two cross-linking agents affect the mechanical properties of collagen fibrils and do this differently. Shen et al. have determined the stress and strain at break for collagen fibrils isolated from sea cucumber dermis (Shen et al., 2008). Fracture strengths of 230 ± 160 MPa and strains of 80% ± 44% were determined. Both the stress and strain at break are significantly higher than as for bovine type collagen. Differences in the amount of crosslinking (not mentioned in Shen et al., 2008) and the collagen being of a different origin, can explain the differences in properties.

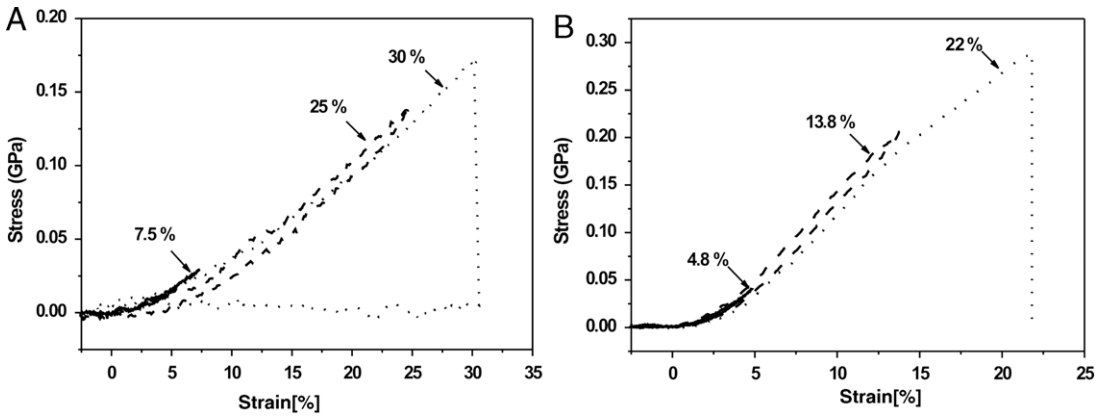

Fig. 4 – Representative stress–strain curves of an individual collagen type I fibril cross-linked by EDC/NHS (A) or glutaraldehyde (B) in PBS buffer. Stretching and relaxation cycles of the fibril up to different percentages of strain are indicated. The strain rate for all stretching-relaxation cycles is 4 μm/s. For (A), failure of the fibril occurred at 30% strain with a stress of 0.17 GPa (dotted line) in PBS buffer. The fibril immersed in PBS buffer is 53 ± 2 μm in length and 300 ± 10 nm in diameter. For (B), failure of the fibril occurred at 22% strain with a stress of 0.29 GPa (dotted line) in PBS buffer. The fibril immersed in PBS buffer is 90 ± 2 μm in length and 295 ± 14 nm in diameter.

Table 1 – Mechanical properties of individual collagen fibrils immersed in PBS buffer (from tensile tests at strain rate 4 μm/s). Values are means ± SD.

	In PBS buffer			
	E (GPa)[a]	σ_c (GPa)[b]	σ_{max} (GPa)	ε_{max} (%)
Native fibrils	0.6 ± 0.2	0.02 ± 0.01	0.06 ± 0.01	13 ± 2
Fibrils crosslinked with EDC/NHS	0.7 ± 0.1	0.06 ± 0.01	0.17 ± 0.01	30 ± 3
Fibrils crosslinked with glutaraldehyde	1.8 ± 0.3	0.15 ± 0.02	0.29 ± 0.01	22 ± 3

[a]Moduli were determined from the maximum slope of the stress–strain curve of single collagen fibrils.
[b]The stress for the transition from reversible to irreversible lengthening of the fibril.

3.4. *Strain rate dependency*

For tendons and ligaments it is known that the mechanical behavior depends on the rate of the applied strain (Haut and Haut, 1997; Usha et al., 2001; Lynch et al., 2003; Robinson et al., 2004; Komatsu et al., 2004; Wu et al., 2006; Wu, 2006). This indicates viscoelastic behavior, which may result both from the interaction between proteoglycans and collagen in tissues and from collagen itself (Screen et al., 2004). For collagen fibrils loaded to relatively high stresses, hysteresis and irreversible lengthening were observed, both indicative of viscoelastic properties. In the following, the strain rate dependence of the stress–strain behavior and the stress-relaxation behavior of single collagen fibrils will be discussed.

A selected collagen fibril was fixed between an AFM cantilever and a glass surface and stretched at different rates ranging from 0.1 to 10 μm/s. The typical stress–strain behavior of the fibrils in PBS buffer at strain rates of 0.1 μm/s, 1 μm/s and 10 μm/s is shown in Fig. 5(A)–(C). Experiments on (non)cross-linked collagen fibrils immersed in PBS buffer showed a ~30% increase in the elasticity modulus by increasing the strain rate a 100 times. Stretching the collagen fibril multiple times at one of the selected strain rates, did not show significant differences in the stress–strain behavior (difference in modulus <5%, data not shown). This clearly shows that earlier performed tensile tests had no significant influence on the mechanical properties of the fibril in the range of strain applied.

3.5. *Stress relaxation behavior*

The stress relaxation behavior of collagen fibrils was studied by extending the collagen fibrils to 5%–7% strain and measuring the force at constant strain for a 5–10 min period. The normalized stress $\sigma(t)/\sigma(0)$ against time gave stress relaxation curves for native and cross-linked collagen fibrils immersed in PBS buffer as depicted in Fig. 5(D)–(F). All samples relaxed rapidly at first and then progressively slower thereafter.

The Maxwell models with one, two or three terms (Eq. (2)), also known as the Prony series, were used to fit the stress relaxation data. Using the quality of the fit, expressed as the coefficient of determination (R2) as a parameter, the two-term Maxwell model fitted the data most accurately. The fitted curves are plotted in Fig. 5(D)–(F). The relaxation times resulting from the curve-fitting are presented in Table 2. It is noteworthy to mention that a two-term Prony series that was initially used for rubber modified polymers, has also been used to describe the relaxation behavior of tendon collagen fibers and soft tissues such as skin (Wu et al., 2006).

The almost two orders of magnitude difference in τ_1 and τ_2 indicate that there are two distinct processes involved in the relaxation of individual collagen fibrils, a fast τ_1 and slow τ_2

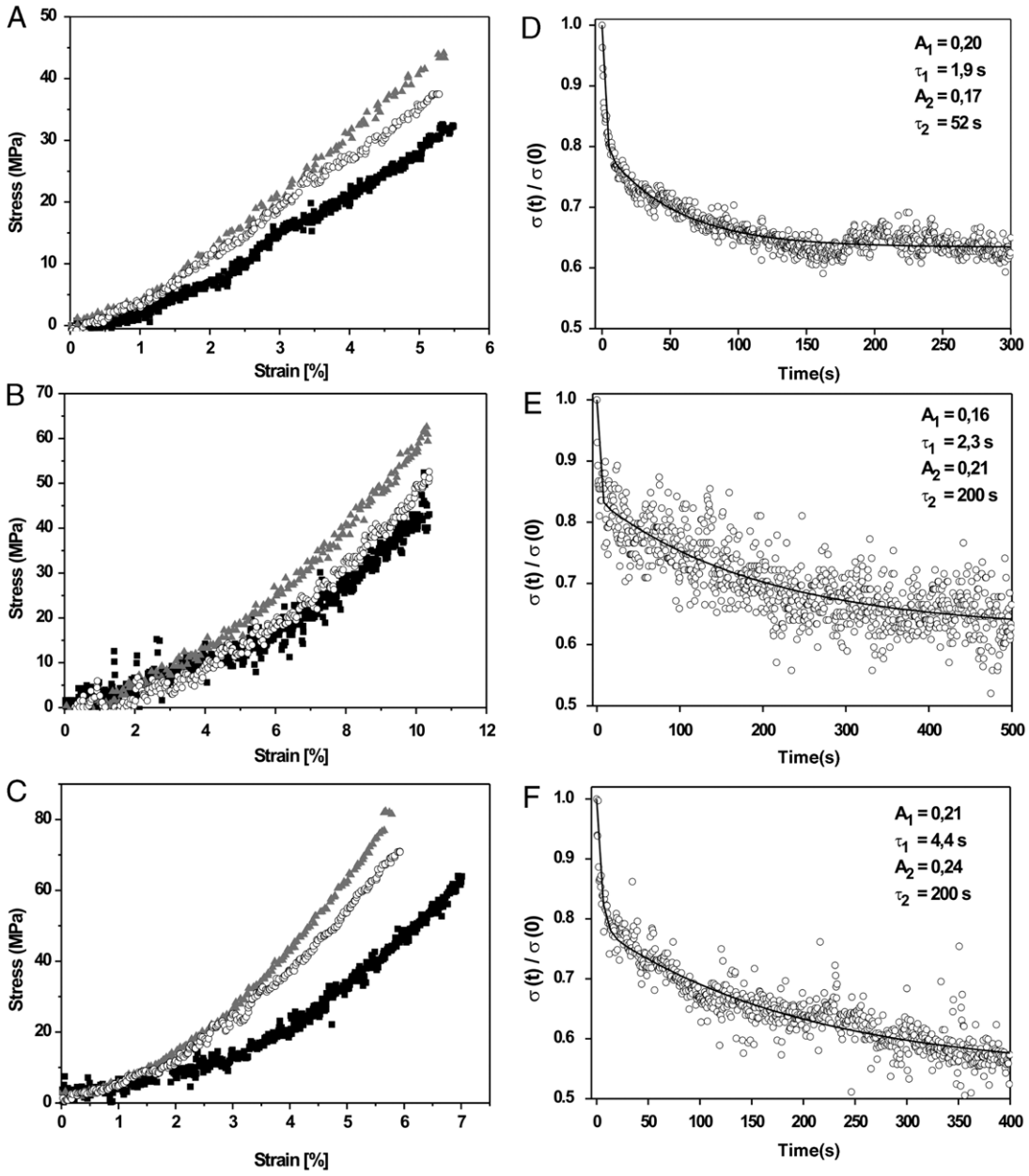

Fig. 5 – (A)–(C) Examples of stress–strain responses of individual native collagen fibrils (A), EDC/NHS cross-linked fibrils (B), and glutaraldehyde cross-linked fibrils (C) immersed in PBS buffer at strain rates of 0.1 μm/s (filled squares), 1.0 μm/s (open circles) and 10 μm/s (triangles). (D)–(F) Normalized stress relaxation curves of individual native collagen fibrils (D), EDC/NHS cross-linked collagen fibrils (E) and glutaraldehyde cross-linked collagen fibrils (F) immersed in PBS buffer. The data (open circles) were curve fitted to Eq. (2) using 2 terms (fitting: solid lines).

relaxation. For native fibrils a fast relaxation time of 1.8 s and a slow component with a typical time constant of 63 s was found. Eppell and coworkers have measured collagen fibrils isolated from sea cucumbers using a MEMS device and found also two time components, namely 7 s for the fast relaxation component and 102 s for the slow component (Shen et al., 2011).

As can be read in Table 2, different cross-linking agents affect the relaxation times of the collagen fibrils differently. For collagen fibrils cross-linked with glutaraldehyde, both relaxation times τ_1 and τ_2 were found to be significantly higher, compared to those of native fibrils, whilst for EDC/NHS cross-linked collagen fibrils only the slower component τ_2 was affected. These differences in the stress relaxation behavior must be related to the differences in the type of cross-links formed by glutaraldehyde and EDC/NHS. Glutaraldehyde cross-linking enables covalent binding of two amine groups of (hydroxy)-lysine residues at a distance of 1.3 nm (Olde Damink et al., 1995). The distance between microfibrils as calculated from the triple helix backbone is 1.3–1.7 nm (Ramachandran, 1967). Therefore, it is expected that glutaraldehyde cross-links generate intra- and inter-

Table 2 – Characteristic relaxation times derived from curve-fitting the force relaxation as a function of time with a two-term Prony series. Each value (mean ± S.D.) results from measurements of 3 individual fibrils.

Relaxation time (s)	Native[a]	EDC/NHS[b]	Glutaraldehyde[c]
τ_1	1.8 ± 0.2	2.0 ± 0.6	3.7 ± 0.6
τ_2	63 ± 23	216 ± 10	252 ± 82

[a]Native collagen fibrils.
[b]Collagen fibrils cross-linked by EDC/NHS.
[c]Collagen fibrils cross-linked by glutaraldehyde.

molecular cross-links as well as inter-microfibrillar cross-links. However, "zero-length" amide and ester cross-links are formed using EDC/NHS (Olde Damink et al., 1996; Everaerts et al., 2007). In the latter case only intra- and inter-molecular cross-links can be formed and cross-links between microfibrils are absent.

3.6. *Proposed model for the stress relaxation of individual collagen fibrils*

The sliding of collagen fibrils has proven to be the major mechanism for the viscoelastic mechanical properties of tendon (Screen et al., 2004). A similar mechanism can be responsible for the viscoelastic properties observed on the level of the individual collagen fibril. Within the collagen fibrillar structure, the collagen molecule is regarded as an elastic rod (Engel, 1997). The viscoelastic behavior of a collagen fibril can be explained by the sliding of individual collagen molecules as well as the sliding of collagen microfibrils with respect to each other.

Using tensile testing combined with synchrotron radiation diffraction for tissue samples, Mosler and co-workers reported that there are two mechanisms that contribute to the elongation of collagen fibrils, namely the stretching of the collagen molecules and their sliding with respect to each other. By applying a constant load, the continuous change in the intensity of the diffraction spectra up to 200 s indicated that sliding of the molecules takes place, which can be attributed to the viscous behavior of the collagen fibril (Mosler et al., 1985). From the stress relaxation measurements on rat tail tendon, Usha et al. (2001) suggested that the relaxation time in the order of 200 s was related to the sliding between collagen molecules which was hindered by hydrogen bonding. In our research, by applying a constant strain, a continuous decay in stress with a fast and slow relaxation process (τ_1 and τ_2) was observed. The slow relaxation process with a characteristic time τ_2 of 63 s for native collagen fibrils can be related to the sliding between the molecules. Upon cross-linking either with EDC/NHS or glutaraldehyde, additional intra- and inter-molecular cross-links are introduced. The additional crosslinks will hinder the sliding of the molecules, which explains the increase of τ_2 to ~216 s and 252 s for cross-linked collagen fibrils.

Moreover, our results indicate that there is a second viscous element with a shorter characteristic time τ_1 contributing to the viscoelastic behavior of collagen fibrils. This sliding behavior will occur at all hierarchical levels within the collagen fibril but predominantly between units exhibiting the weakest interaction. In native collagen type I fibrils, molecules are cross-linked at the telopeptide region (Folkhard et al., 1987a). However, there are only a few cross-links present between microfibrils, which are assemblies of five collagen molecules (Orgel et al., 2006). Based on these results, it is hypothesized that sliding between microfibrils is the viscous element responsible for the fast relaxation component during the stress relaxation process. This hypothesis is further supported by the data of the stress relaxation experiments with the different cross-linkers. Collagen fibrils cross-linked by glutaraldehyde likely contain also cross-links between microfibrils resulting in a clear increase in the value of the slow relaxation time τ_1. EDC/NHS cross-linking, however, which is a "zero-length" cross-linker did not affect the value of τ_1. This difference can be related to the formation of cross-links between collagen molecules but not between microfibrils, since the distance between collagen microfibrils is too large. The sliding between collagen microfibrils is one of the mechanisms which introduces a rapid and significant decay of stress in the stress relaxation process. The sliding between collagen molecules, limited by the natural cross-linking at the telopeptide region, proceeds more slowly with relaxation times in the range 60–250 s. Based on electron density maps of collagen, Orgel et al. (2006), proposed a topologically right-handed supertwisted microfibrillar structure in collagen fibrils. As they mentioned in their model, this supertwisted microfibrillar structure may allow the structure to absorb torsion effects without interfering with the superhelix of the collagen molecule itself. This can also be the reason for the much slower sliding of collagen molecules with respect to each other compared to the sliding of microfibrils with respect to each other.

In our previous work (Yang et al., 2008), we found that the shear modulus of single collagen fibrils was two orders of magnitude lower than the elasticity modulus, confirming the mechanical anisotropy of single collagen fibrils. The shear moduli for native and EDC/NHS cross-linked collagen fibrils placed in buffer were found to be similar, supporting the explanation that the sliding of microfibrils with respect to each other is probably the main factor influencing the shear modulus of single collagen fibrils, and to a lesser degree the sliding of individual collagen molecules. In this study, the results on the stress relaxation behavior of native and cross-linked collagen fibrils further supported the existence of a microfibrillar structure and the role of microfibrils in the mechanical behavior of single collagen fibrils.

4. Conclusions

In conclusion, using an atomic force microscope we have performed tensile tests at various strain rates and stress relaxation experiments on native collagen fibrils isolated from bovine Achilles tendon and collagen fibrils cross-linked with different cross-linking agents to study the relationship between the fibril structure and its mechanical behavior. The stress–strain behavior, elasticity modulus and the failure stress and strain of individual collagen fibrils immersed in PBS buffer were determined for the first time.

A two-term Prony series was used to curve-fit the stress relaxation behavior of native and cross-linked collagen fibrils. The results indicate that there are two distinct processes contributing to the stress relaxation behavior of collagen fibrils: a fast relaxation process with a characteristic time τ_1 and a slow relaxation process with characteristic time τ_2. The relaxation times were influenced differently by the cross-linkers EDC/NHS and glutaraldehyde. Based on these results, it is proposed that the fast relaxation τ_1 is related to the sliding of collagen microfibrils with respect to each other, as the slow relaxation τ_2 is resulting from the sliding of molecules with respect to each other. The sliding of microfibrils requires less energy because of the lower number of cross-links between microfibrils as compared to collagen molecules. As a result the sliding of microfibrils is much faster than that of the collagen molecules. This study together with our previous work supports the existence of microfibrils and the role of such structures in the mechanical behavior of single collagen fibrils.

Acknowledgments

This research was financially supported by the Softlink program of ZonMw. Project number: 01SL056.

REFERENCES

An, K.N., Sun, Y.L., Luo, Z.P., 2004. Flexibility of type I collagen and mechanical property of connective tissue. Biorheology 41, 239–246.

Baselt, D.R., Revel, J.P., Baldeschwieler, J.D., 1993. Subfibrillar structure of type I collagen observed by atomic force microscopy. Biophys. J. 65, 2644–2655.

Buehler, M.J., 2006. Nature designs tough collagen: explaining the nanostructure of collagen fibrils. Proc. Natl. Acad. Sci. USA 103, 12285–12290.

Buehler, M.J., 2008. Nanomechanics of collagen fibrils under varying cross-link densities: atomistic and continuum studies. J. Mech. Behav. Biomed. Mater. 1, 59–67.

Butler, D.L., Kay, M.D., Stouffer, D.C., 1986. Comparison of material properties in fascicle-bone units from human patellar tendon and knee ligaments. J. Biomech. 19, 425–432.

Carrion-Vazquez, M., Oberhauser, A.F., Fisher, T.E., Marszalek, P.E., Li, H., Fernandez, J.M., 2000. Mechanical design of proteins studied by single-molecule force spectroscopy and protein engineering. Prog. Biophys. Mol. Biol. 74, 63–91.

Dowling, B.A., Dart, A.J., 2005. Mechanical and functional properties of the equine superficial digital flexor tendon. Vet. J. 170, 184–192.

Engel, J., 1997. Versatile collagens in invertebrates. Science 277, 1785–1786.

Eppell, S.J., Smith, B.N., Kahn, H., Ballarini, R., 2006. Nano measurements with micro-devices: mechanical properties of hydrated collagen fibrils. J. R. Soc. Interface 3, 117–121.

Everaerts, F., Torrianni, M., Hendriks, M., Feijen, J., 2007. Quantification of carboxyl groups in carbodiimide cross-linked collagen sponges. J. Biomed. Mater. Res. Part A 83, 1176–1183.

Fisher, T.E., Oberhauser, A.F., Carrion-Vazquez, M., Marszalek, P.E., Fernandez, J.M., 1999. The study of protein mechanics with the atomic force microscope. Trends Biochem. Sci. 24, 379–384.

Folkhard, W., Geercken, W., Knörzer, E., Mosler, E., Nemetschek-Gansler, H., Nemetschek, Th., 1987b. Structural dynamic of native tendon collagen. J. Mol. Biol. 193, 405–407.

Folkhard, W., Mosler, E., Geercken, W., Knörzer, E., Nemetschek-Gansler, H., Nemetschek, Th., Koch, M.H.J., 1987a. Quantitative analysis of the molecular sliding mechanism in native tendon collagen—time-resolved dynamic studies using synchrotron radiation. Int. J. Biol. Macromol. 9, 169–175.

Gautieri, A., Vesentini, S., Redaelli, A., Buehler, M.J., 2011. Hierarchical structure and nanomechanics of collagen microfibrils from the atomistic scale up. Nano Lett. 11, 757–766.

Graham, J.S., Vomund, A.N., Phillips, C.L., Grandbois, M., 2004. Structural changes in human type I collagen fibrils investigated by force spectroscopy. Exp. Cell Res. 299, 335–342.

Guzmán, C., Jeney, S., Kreplak, L., Kasas, S., Kulik, A.J., Aebi, U., Forró, L., 2006. Exploring the mechanical properties of single vimentin intermediate filaments by atomic force microscopy. J. Mol. Biol. 360, 623–630.

Habelitz, S., Balooch, M., Marshall, S.J., Balooch, G., Marshall, G.W., 2002. In situ force microscopy of partially demineralized human dentin collagen fibrils. J. Struct. Biol. 138, 227–236.

Haut, T.L., Haut, R.C., 1997. The state of tissue hydration determines the strain-rate-sensitive stiffness of human patellar tendon. J. Biomech. 30, 79–81.

Holmes, D.F., Gilpin, C.J., Baldock, C., Ziese, U., Koster, A.J., Kadler, K.E., 2001. Corneal collagen fibril structure in three dimensions: structural insights into fibril assembly, mechanical properties, and tissue organization. Proc. Natl. Acad. Sci. USA 98, 7307–7312.

Hulmes, D.J.S., 2002. Building collagen molecules, fibrils, and suprafibrillar structures. J. Struct. Biol. 137, 2–10.

Kis, A., Kasas, S., Babić, B., Kulik, A.J., Benoît, W., Briggs, G.A.D., Schönenberger, C., Catsicas, S., Forró, L., 2002. Nanomechanics of microtubules. Phys. Rev. Lett. 89, 248101.

Komatsu, K., Kanazashi, M., Shimada, A., Shibata, T., Viidik, A., Chiba, M., 2004. Effects of age on the stress–strain and stress-relaxation properties of the rat molar periodontal ligament. Arch. Oral Biol. 49, 817–824.

Lynch, H.A., Johannessen, W., Wu, J.P., Jawa, A., Elliott, D.M., 2003. Effect of fiber orientation and strain rate on the nonlinear uniaxial tensile material properties of tendon. J. Biomech. Eng. 125, 726–731.

Magnusson, S.P., Hansen, P., Kjaer, M., 2003. Tendon properties in relation to muscular activity and physical training. Scand. J. Med. Sci. Sports 13, 211–223.

Misof, K., Rapp, G., Fratzl, P., 1997. A new molecular model for collagen elasticity based on synchrotron X-ray scattering evidence. Biophys. J. 72, 1376–1381.

Mosler, E., Folkhard, W., Knörzer, E., Nemetschek-Gansler, H., Nemetschek, Th., Koch, M.H.J., 1985. Stress-induced molecular rearrangement in tendon collagen. J. Mol. Biol. 182, 589–596.

Olde Damink, L.H.H., Dijkstra, P.J., van Luyn, M.J.A., van Wachem, P.B., Nieuwenhuis, P., Feijen, J., 1995. Glutaraldehyde as a crosslinking agent for collagen-based biomaterials. J. Mater. Sci. Mater. Med. 6, 460–472.

Olde Damink, L.H.H., Dijkstra, P.J., van Luyn, M.J.A., van Wachem, P.B., Nieuwenhuis, P., Feijen, J., 1996. Cross-linking of dermal sheep collagen using a water-soluble carbodiimide. Biomaterials 17, 765–773.

Oliver, W.C., Pharr, G.M., 2004. Measurement of hardness and elastic modulus by instrumented indentation: advances in understanding and refinement to methodology. J. Mater. Res. 19, 3–20.

Orgel, J.P.R.O., Irving, T.C., Miller, A., Wess, T.J., 2006. Microfibrillar structure of type I collagen in situ. Proc. Natl. Acad. Sci. USA 103, 9001–9005.

Ottani, V., Martini, D., Franchi, M., Ruggeri, A., Raspanti, M., 2002. Hierarchical structures in fibrillar collagens. Micron 33, 587–596.

Pins, G.D., Silver, F.H., 1995. A self-assembled collagen scaffold suitable for use in soft and hard tissue replacement. Mater. Sci. Eng. C 3, 101–107.

Puxkandl, R., Zizak, I., Paris, O., Keckes, J., Tesch, W., Bernstorff, S., Purslow, P., Fratzl, P., 2002. Viscoelastic properties of collagen: synchrotron radiation investigations and structural model. Philos. Trans. R. Soc. Lond. Ser. B 357, 191–197.

Ramachandran, G.N., 1967. Structure of Collagen at a Molecular Level. Academic Press, London.

Raspanti, M., Congiu, T., Guizzardi, S., 2001. Tapping-mode atomic force microscopy in fluid of hydrated extracellular matrix. Matrix Biol. 20, 601–604.

Robinson, P.S., Lin, T.W., Reynolds, P.R., Derwin, K.A., Iozzo, R.V., Soslowsky, L.J., 2004. Strain-rate sensitive mechanical properties of tendon fascicles from mice with genetically engineered alterations in collagen and decorin. J. Biomech. Eng. 126, 252–257.

Sasaki, N., Odajima, S., 1996. Elongation mechanism of collagen fibrils and force–strain relations of tendon at each level of structural hierarchy. J. Biomech. 29, 1131–1136.

Screen, H.R.C., Lee, D.A., Bader, D.L., Shelton, J.C., 2004. An investigation into the effects of the hierarchical structure of tendon fascicles on micromechanical properties. Proc. Inst. Mech. Eng. H. 218, 109–119.

Shen, Z.L., Dodge, M.R., Kahn, H., Ballarini, R., Eppell, S.J., 2008. Stress–strain experiments on individual collagen fibrils. Biophys. J. 95, 3956–3963.

Shen, Z.L., Kahn, H., Ballarini, R., Eppell, S.J., 2011. Viscoelastic properties of isolated collagen fibrils. Biophys. J. 100, 3008–3015.

Silver, F.H., Christiansen, D., Snowhill, P.B., Chen, Y., Landis, W.J., 2000. The role of mineral in the storage of elastic energy in turkey tendons. Biomacromolecules 1, 180–185.

Silver, F.H., Freeman, J.W., Seehra, G.P., 2003. Collagen self-assembly and the development of tendon mechanical properties. J. Biomech. 36, 1529–1553.

Smith, J.W., 1968. Molecular pattern in native collagen. Nature 219, 157–158.

Smith, J.F., Knowles, T.P.J., Dobson, C.M., Macphee, C.E., Welland, M.E., 2006. Characterization of the nanoscale properties of individual amyloid fibrils. Proc. Natl. Acad. Sci. USA 103, 15806–15811.

Strasser, S., Zink, A., Janko, M., Heckl, W.M., Thalhammer, S., 2007. Structural investigations on native collagen type I fibrils using AFM. Biochem. Biophys. Res. Commun. 354, 27–32.

Svennson, R.B., Hassenkam, T., Grant, C.A., Magnusson, S.P., 2010. Tensile properties of human collagen fibrils and fascicles are insensitive to environmental salts. Biophys. J. 99, 4020–4027.

Svensson, R.B., Hassenkam, T., Hansen, P., Magnusson, S.P., 2010. Viscoelastic behavior of discrete human collagen fibrils. J. Mech. Behav. Biomed. Mater. 3, 112–115.

Thompson, J.B., Kindt, J.H., Drake, B., Hansma, H.G., Morse, D.E., Hansma, P.K., 2001. Bone indentation recovery time correlates with bond reforming time. Nature 414, 773–776.

Torii, A., Sasaki, M., Hane, K., Okuma, S., 1996. A method for determining the spring constant of cantilevers for atomic force microscopy. Meas. Sci. Technol. 7, 179–184.

Usha, R., Subramaniam, V., Ramasami, T., 2001. Role of secondary structure on the stress relaxation processes in rat tail tendon (RTT) collagen fibre. Macromol. Biosci. 1, 100–107.

van der Rijt, J.A.J., van der Werf, K.O., Bennink, M.L., Dijkstra, P.J., Feijen, J., 2006. Micromechanical testing of individual collagen fibrils. Macromol. Biosci. 6, 697–702.

Wang, J.H.C., 2006. Mechanobiology of tendon. J. Biomech. 39, 1563–1582.

Wenger, M.P.E., Bozec, L., Horton, M.A., Mesquida, P., 2007. Mechanical properties of collagen fibrils. Biophys. J. 93, 1255–1263.

Wineman, A.S., Rajagopal, K.R., 2000. Mechanical Response of Polymers: An Introduction. Cambridge University Press, New York.

Wu, J.J., 2006. Quantitative constitutive behaviour and viscoelastic properties of fresh flexor tendons. Int. J. Artif. Organs 29, 852–857.

Wu, J.Z., Cutlip, R.G., Welcome, D., Dong, R.G., 2006. Estimation of the viscous properties of skin and subcutaneous tissue in uniaxial stress relaxation tests. Biomed. Mater. Eng. 16, 53–66.

Yang, L., van der Werf, K.O., Fitié, C.F.C., Bennink, M.L., Dijkstra, P.J., Feijen, J., 2008. Mechanical properties of native and cross-linked type I collagen fibrils. Biophys. J. 94, 2204–2211.

Yang, L., van der Werf, K.O., Koopman, B.F.J.M., Subramaniam, V., Bennink, M.L., Dijkstra, P.J., Feijen, J., 2007. Micromechanical bending of single collagen fibrils using atomic force microscopy. J. Biomed. Mater. Res. Part A 82, 160–168.